pss +++rapid research letters +++

www.pss-rapid.com

Imaging of the interstitial iron concentration in crystalline silicon by measuring the dissociation rate of iron–boron pairs

Sandra Herlufsen[*, 1], **Daniel Macdonald**[2], **Karsten Bothe**[1], **and Jan Schmidt**[1]

[1] Institute for Solar Energy Research Hamelin (ISFH), Am Ohrberg 1, 31860 Emmerthal, Germany
[2] Research School of Engineering, The Australian National University, Canberra, ACT 0200, Australia

[*] Corresponding author: e-mail herlufsen@isfh.de, Phone: +49-5151-999-414, Fax: +49-5151-999-400

We present a dynamic approach for measuring the interstitial iron concentration in boron-doped crystalline silicon using photoluminescence (PL) imaging. This camera-based technique utilizes the characteristic dependence of the dissociation rate of iron–boron pairs on the interstitial iron concentration. We determine the dissociation rate by measuring the time-dependent PL signal after complete association of iron–boron pairs in the sample. Since we are only interested in the time dependence of the PL signal, we are able to generate images of the interstitial iron concentration in absolute units without any calibration and without knowing the recombination properties of the interstitial iron or iron–boron pairs.

Iron is a well-known and detrimental impurity in crystalline silicon (c-Si) for solar cells [1], especially in block-cast multicrystalline silicon (mc-Si). So far, most measurement techniques used to determine the spatial distribution of interstitial iron (Fe_i) in B-doped silicon wafers are based on measurements of the carrier lifetimes or diffusion lengths before and after iron–boron (FeB) pair dissociation [2–4]. The result of these lifetime-based techniques depends crucially on the knowledge of the recombination properties of Fe_i and FeB. If camera-based photoluminescence (PL) measurements [5] are used to determine the spatially resolved carrier lifetime, rapid generation of images of the Fe_i concentration is possible [6]. In PL measurements, the Fe_i concentration is typically investigated under low-level injection conditions. In this case, the Fe_i concentration, calculated from absolute lifetime values, is very sensitive to the exact value of the electron capture cross section of Fe_i, a parameter which is not well known [3, 6–8]. In this Letter, we propose a technique for the determination of the Fe_i concentration in B-doped c-Si that measures the dissociation rate of FeB pairs using a PL camera signal. This approach enables us to identify the Fe_i concentration without measuring absolute values of the carrier lifetime and without knowing the recombination

properties of Fe_i and FeB in Si. Hence, an extra calibration of the PL signal to the excess carrier density is not required. We take advantage of the dependence of the dissociation rate on the Fe_i concentration [10] and the linear relationship that exists between the excess carrier density and photoluminescence signal at low injection levels. Therefore, we need only record the time-dependence of the uncalibrated PL signal during constant photogeneration.

In previous techniques, the interstitial iron concentration $[Fe_i]$ of passivated B-doped Si wafers was mostly determined by measuring absolute values of the carrier lifetime τ with the Fe_i in two different states, namely (i) τ_{FeB}, when the Fe_i is bound to B dopant atoms to form FeB pairs and (ii) τ_{Fe_i}, after complete dissociation of the FeB pairs. Due to the different recombination properties of the iron in these two states, the Fe_i concentration can be deduced from the difference of the inverse bulk lifetimes [3, 4]:

$$[Fe_i] = C_{SRH} \left(\frac{1}{\tau_{Fe_i}} - \frac{1}{\tau_{FeB}} \right), \tag{1}$$

with C_{SRH} being a prefactor which depends on the doping and excess carrier concentration [4]. Geerligs et al. investigated the dynamics of light-induced FeB pair dissociation
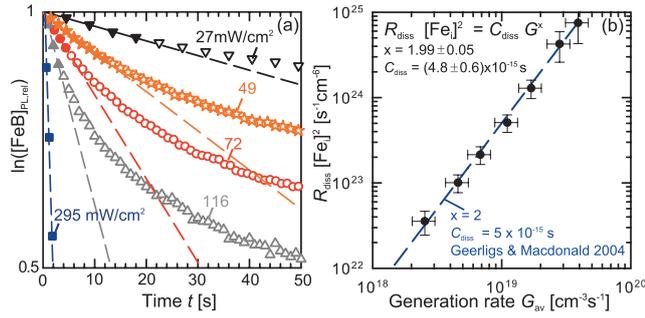
Figure 1 (online colour at: www.pss-rapid.com) (a) Natural logarithm of [FeB]$_{PL,rel}$ in dependence on time t for different laser illumination intensities for a deliberately Fe-contaminated B-doped FZ-Si wafer with [Fe$_i$] = 2.5×10^{12} cm^{-3}. The filled symbols show the data points that are used for the linear regression (dashed lines). (b) Product of the measured R_{diss} of Fig. 1(a) and [Fe$_i$]^2 in dependence on the average generation rate G_{av}. The blue dashed line shows the dependence obtained in Ref. [10].

and revealed a quadratic dependence of the dissociation rate R_{diss} on the average photogeneration rate G_{av} and an inverse proportionality on the square of the interstitial iron concentration [Fe$_i$] [10]:

$$R_{diss} = C_{diss} \frac{G_{av}^2}{[Fe_i]^2} , \qquad (2)$$

with a proportionality constant C_{diss} that Geerligs et al. [10] determined to be $C_{diss} = 5 \times 10^{-15}$ s. As described in Ref. [10] R_{diss} can be easily obtained by linear regression of the derivative of the natural logarithm of the FeB pair concentration [FeB]$_{rel}$, normalized with respect to the total FeB concentration at $t = 0$:

$$\left. \frac{d\left[\ln\left([FeB]_{rel}\right)\right]}{dt} \right|_{t=0} = -R_{diss} . \qquad (3)$$

Equation (3) is valid for $t = 0$ or at least: $t < (R_{rep} + R_{diss})^{-1}$ with R_{rep} being the re-pairing rate of FeB pairs [11]. At low injection levels, the measured PL signal I_{PL} is, within limits [12], proportional to the excess carrier density. Hence, for a constant photogeneration rate, I_{PL} is proportional to the carrier lifetime. Using this knowledge and Eq. (1), we are able to calculate the relative FeB concentration [FeB]$_{PL,rel}(t)$ using only measured PL signals without requiring an additional calibration technique:

$$[FeB]_{PL,rel}(t) \propto \frac{1}{I_{PL,Fe_i}} - \frac{1}{I_{PL,FeB}(t)} , \qquad (4)$$

with I_{PL,Fe_i} being the PL signal measured for the dissociated state of the FeB pairs, and $I_{PL,FeB}(t)$ being the time-dependent PL signal after complete FeB pair association during constant photogeneration.

Technical details of our camera-based PL setup have been published elsewhere [9, 13]. In this study, the associated state of the Fe$_i$ with the substitutional boron is ob-

tained by placing the sample on a hotplate at 50 °C for about 30 min. After complete association of the FeB pairs, we record a sequence of PL images for the determination of [FeB]$_{PL,rel}(t)$. Between the acquisitions of the PL images, the light source is off. This time in the dark can be neglected in the evaluation since the fraction that re-pairs during that time is negligible compared to the dissociated fraction. The PL signal of the fully dissociated state is measured after exposing the wafer to about 15 flashes of a photo flashlamp with an intensity of up to 100 W/cm^2. All PL measurement were performed at a sample temperature of 25 °C. We use a calibrated Si solar cell to measure the photon flux φ_{laser} during illumination with a laser. The average generation rate for excess carriers G_{av} in a Si wafer of thickness W and reflectivity at the excitation wavelength R_{laser} is then calculated using $G_{av} = \varphi_{laser}(1 - R_{laser})/W$.

We verify the results of Geerligs et al. [10] by measuring the time-dependence of [FeB]$_{PL,rel}$ for different illumination intensities for a deliberately Fe-contaminated SiN$_x$-passivated float-zone (FZ) Si wafer with a resistivity of 1 Ω cm, a thickness of 385 μm and [Fe$_i$] = 2.5×10^{12} cm^{-3}. The iron was introduced by ion implantation and the Fe$_i$ concentration was deduced from the implanted Fe dose. Details of the sample preparation have been published elsewhere [14]. The dissociation rate of FeB pairs R_{diss} is determined from [FeB]$_{PL,rel}$ by linear regression of ln ([FeB]$_{PL,rel}$) using Eq. (3). Figure 1(a) shows ln ([FeB]$_{PL,rel}$) as a function of time for different illumination intensities, expressed in units of mW/cm^2. To increase the signal-to-noise ratio, we averaged the PL signal over an area of about 2 cm^2 for the data in Fig. 1(a). In Fig. 1(b), the product of R_{diss}, as obtained from our PL measurements, and [Fe$_i$]^2, as calculated from the implanted dose, is plotted on a double logarithmic scale against the measured photogeneration rate G_{av}. The dashed blue line shows the dependence published by Geerligs and Macdonald [10]. The excellent agreement further justifies using Eq. (2) for the dynamic determination of the interstitial iron concentration [Fe$_i$]$_{dyn}$ by measuring the dissociation rate R_{diss} of the FeB pairs.
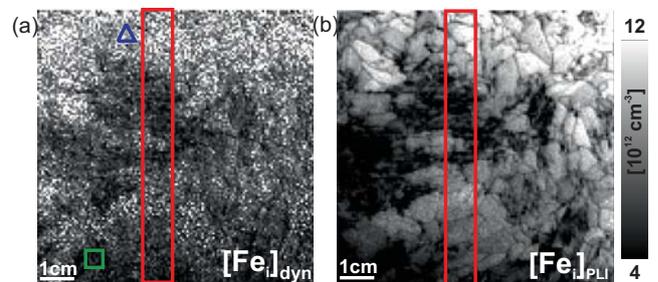
Figure 2 (online colour at: www.pss-rapid.com) Spatially resolved interstitial iron concentration [Fe$_i$] for a wafer from the top region of a mc-Si ingot, determined from (a) the dissociation rate R_{diss} of FeB pairs ([Fe$_i$]$_{dyn}$) and from (b) calibrated PL lifetime images ([Fe$_i$]$_{PLI}$) [6, 9].
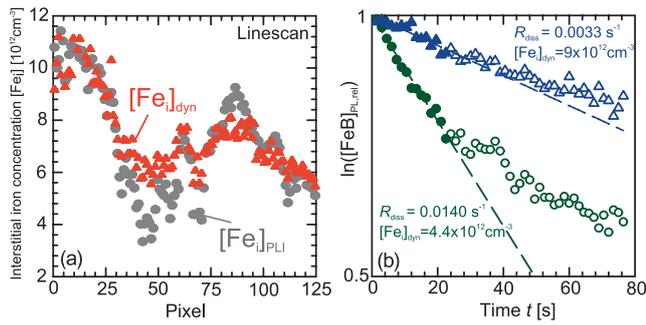
Figure 3 (online colour at: www.pss-rapid.com) (a) Linescan, averaged over 12 pixel rows, marked in Fig. 2 with a red rectangle, for $[Fe_i]_{dyn}$ and $[Fe_i]_{PLI}$. (b) Natural logarithm of $[FeB]_{rel.PL}(t)$ in dependence on time for two different regions, marked in Fig. 2 with a blue triangle and a green square, with different R_{diss} and therefore different $[Fe_i]$. The dashed lines show the linear regressions for $t < (R_{rep} + R_{diss})^{-1}$.

We demonstrate the applicability of our dynamic approach for measuring $[Fe_i]_{dyn}$ by investigating a solar-grade SiN_x-passivated mc-Si wafer with a resistivity of 0.4 Ω cm and a thickness of 170 μm. The measured $[Fe_i]_{dyn}$ image is shown in Fig. 2(a). For comparison, we show in Fig. 2(b) the calculated interstitial iron concentration $[Fe_i]_{PLI}$ from calibrated PL lifetime images [6, 9], using $\sigma_{n,Fe_i} = 4 \times 10^{-14}$ cm^2 from Ref. [3]. We use the information from 15 images for the linear regression [Eq. (3)] to determine R_{diss} with a camera integration time for each image of $t_{int} = 1.5$ s and an illumination intensity of 34 mW/cm^2. We averaged two measurements and applied 4×4 binning of the pixels to increase the signal-to-noise ratio. Therefore, the total measurement time is 3 min. For a better quantitative verification, we show a linescan in Fig. 3(a), averaged over 12 pixel rows, from the region marked with a red rectangle in Fig. 2. Figure 3(b) exemplarily shows ln $([FeB]_{PL, rel})(t)$ for two regions of the mc-Si wafer with different $[Fe_i]$, marked in Fig. 2(a) with a green square and a blue triangle, respectively. A comparison of $[Fe_i]_{dyn}$ and $[Fe_i]_{PLI}$ in Figs. 2 and 3(a) shows only deviations in the regions of low $[Fe_i]$.

It should be noted that averaging the time-dependent PL signal over two regions with a highly different $[Fe_i]$, will not result in the arithmetical mean of the dissociation rates R_{diss} of the two regions. The region with the higher R_{diss} (i.e. the area with lower $[Fe_i]$) is overrated if averaging the PL signal over both regions due to the higher lifetime and injection level of that area. This behavior is reversed if the camera integration time t_{int} is larger than R_{diss}^{-1} for the area with low $[Fe_i]$, since then the influence of the region with low Fe_i content on the decay of the averaged $[FeB]_{PL,rel}$ is not detected at all. A solution to this problem could be the calibration of the image of $[FeB]_{PL,rel}$ with the $[Fe_i]_{dyn}$ image in a region of high (homogeneous) $[Fe_i]$. A positive side effect of this calibration would be an increased signal-to-noise ratio of the $[Fe_i]$ image.

In order to ensure the validity of Eq. (4), the prefactor C_{SRH} of Eq. (1) is assumed to be independent of injection level, which is a good approximation for low-level injection conditions about two orders of magnitude below the characteristic crossover point [8, 14]. Since we do not evaluate the entire exponential decay curve of $[FeB]_{PL,rel}(t)$, we only observe small changes in injection level. This leads only to small errors in $[FeB]_{dyn}$ due to an injection-dependent C_{SRH} and lifetime. Only close to the crossover point, the slope of C_{SRH} is too steep to assume a constant C_{SRH}.

The empirical quadratic dependence of R_{diss} on the average photogeneration rate G_{av} in Eq. (2) is related to the recombination rate of the injected excess carriers [10, 15]. Using the actual thickness W of the sample for the determination of G_{av} is only valid if the carrier density profile is nearly homogeneous distributed over the sample depth. For high $[Fe_i]$ and short excitation wavelengths, the excess carriers are rather located close to the surface directed to the excitation. In that case, the definition of G_{av} should be corrected by using an effective thickness W_{eff} as defined by Bowden et al. [16]. If we use W instead of W_{eff}, $[Fe_i]_{dyn}$ would be underestimated. Fortunately, the error is supposed to be small for thin wafers, e.g. for the investigated mc-Si wafer with $W = 170$ μm, the error for $[Fe_i] = 10^{13}$ cm^{-3} would be below 20%.

We have presented a dynamic approach for the determination of the Fe_i concentration in B-doped Si wafers avoiding the necessity of measuring absolute values of the bulk lifetime. By merely detecting the time-dependent PL signal using a camera, we are able to determine the dissociation rate R_{diss} of FeB pairs. We generated an image of the Fe_i concentration of a mc-Si wafer from the measurement of R_{diss} by using its dependence on the Fe_i concentration.

References

[1] A. A. Istratov et al., Appl. Phys. A **70**, 489 (2000).
[2] M. Kittler et al., Phys. Status Solidi A **96**, K133 (1986).
[3] G. Zoth and W. Bergholz, J. Appl. Phys. **11**, 6764 (1990).
[4] D. H. Macdonald et al., J. Appl. Phys. **95**, 1021 (2004).
[5] T. Trupke et al., Appl. Phys. Lett. **89**, 044107 (2006).
[6] D. Macdonald et al., J. Appl. Phys. **103**, 073710 (2008).
[7] S. Rein and S. W. Glunz, J. Appl. Phys. **98**, 113711 (2005).
[8] D. Macdonald et al., Appl. Phys. Lett. **89**, 142107 (2006).
[9] S. Herlufsen et al., Phys. Status Solidi RRL **2**, 245 (2008).
[10] L. J. Geerligs et al., Appl. Phys. Lett. **85**, 5227 (2004).
[11] J. Tan et al., Semicond. Sci. Technol. **26**, 055019 (2011).
[12] T. Trupke, J. Appl. Phys. **100**, 063531 (2006).
[13] D. Hinken et al., Rev. Sci. Instrum. **82**, 033706 (2011).
[14] J. E. Birkholz et al., J. Appl. Phys. **97**, 103708 (2005).
[15] L. C. Kimerling et al., Physica B & C **116B**, 197 (1983).
[16] S. Bowden et al., J. Appl. Phys. **102**, 124501 (2007).